A method for prediction of volcanic eruptions

Barry Voight

Department of Geosciences, The Pennsylvania State University, University Park, Pennsylvania 16802, USA

The relationship $\dot{\Omega}^{-\alpha}\ddot{\Omega} - A = 0$ describes the behaviour of materials in terminal stages of failure, where Ω is an observable quantity such as strain, and A and α are empirical constants. Drawing on analogies between failure mechanics and eruption processes at volcanoes, Ω is interpreted in terms of conventional geodetic, seismic or geochemical observations. Manipulation of Ω provides a consistent analytical basis for eruption prediction.

THE more successful empirical models for predicting volcanic eruptions probably have a common foundation in first principles or natural laws. Although the linkages may seem obscure, theoretical investigations may establish a consistent framework to aid the understanding of empirical relations. Predictions based on such fundamentals are likely to be more reliable than purely probabilistic attempts based on pattern recognition[1]. The purposes of this paper are to: (1) introduce a fundamental relationship describing pre-eruption rate changes of various phenomena; (2) develop equations that couple rate changes of volcanic processes to the time of event occurrence; (3) emphasize the predictive utility of the inverse representation of rate; and (4) apply the predictive method to examples of several specific eruptions.

The basis for the method is the recognition that a fundamental law for failing materials:

$$\dot{\Omega}^{-\alpha}\ddot{\Omega} - A = 0 \qquad (1)$$

where A and α are empirical constants and Ω is an observable quantity, suitably describes the behaviour of many quantities preceding a volcanic eruption[2,3]. The dot refers to differentiation with respect to time. Quantities that might be represented by Ω include strains or displacements for rocks, soils, alloys, metals, plastics, concrete or ice. By encompassing volcanology within the realm of 'rock mechanics', Ω is interpreted in terms of conventional geodetic observations (such as length change, fault slip, strain or angular change), seismic quantities (such as the square root of cumulative energy release) or geochemical observations (such as gas emission rates or chemical ratios) (see Fig. 1).

Volcanic eruptions are invariably preceded and accompanied by rock failure. In volcanic systems, deterministic failure mechanics models may apply to brittle fracture produced in surrounding rock by magma pressure, or by the pressure of volatiles exsolved from magma at various levels, from deep systems ($\geqslant$5 km) to the surficial domes. Dome rupture, conduit clearing or sector collapse influenced by magmatic or volatile pressures all imply damage and stresses in excess of breaking strength. Earthquakes commonly associated with such damage may be 'tectonic-like' (for example, associated with fault slip induced by magmatic pressure), or of the 'shallow-volcanic' or 'surface-event' varieties[4,5]. Gas emission rates and chemical variation may be directly influenced by permeability, pressure and pressure-gradient changes associated with brittle fracture[6,7], and hence may relate to damage-mechanics models.

Theory

Equation (1), a relationship first noted in experimental landslips caused by monotonic load increase[8,9], is perceived as a fundamental physical law governing diverse forms of material failure for conditions of constant stress and temperature[2,3]. If Ω is taken to be strain, for example, the final stages of failure under steady conditions of an alloy in tension, a rock in compression or a tilting volcanic dome would show a proportionality between the logarithm of creep acceleration and the logarithm of creep velocity. Integrating equation (1) gives expressions for the rate, $\dot{\Omega}$. For $\alpha = 1$, and with $\dot{\Omega} = \dot{\Omega}_0$ at $t = t_0$, we have

$$\dot{\Omega} = \dot{\Omega}_0\, e^{A(t-t_0)} \qquad (2)$$

For $\alpha < 1$,

$$\dot{\Omega} = [A(1-\alpha)(t-t_0) + \dot{\Omega}_0^{1-\alpha}]^{1/(1-\alpha)} \qquad (3a)$$

or for $\alpha > 1$,

$$\dot{\Omega} = [A(\alpha-1)(t_f-t) + \dot{\Omega}_f^{1-\alpha}]^{1/(1-\alpha)} \qquad (3b)$$

where t_f is the time of failure and $\dot{\Omega}_f$ the rate at failure (see Fig. 2).

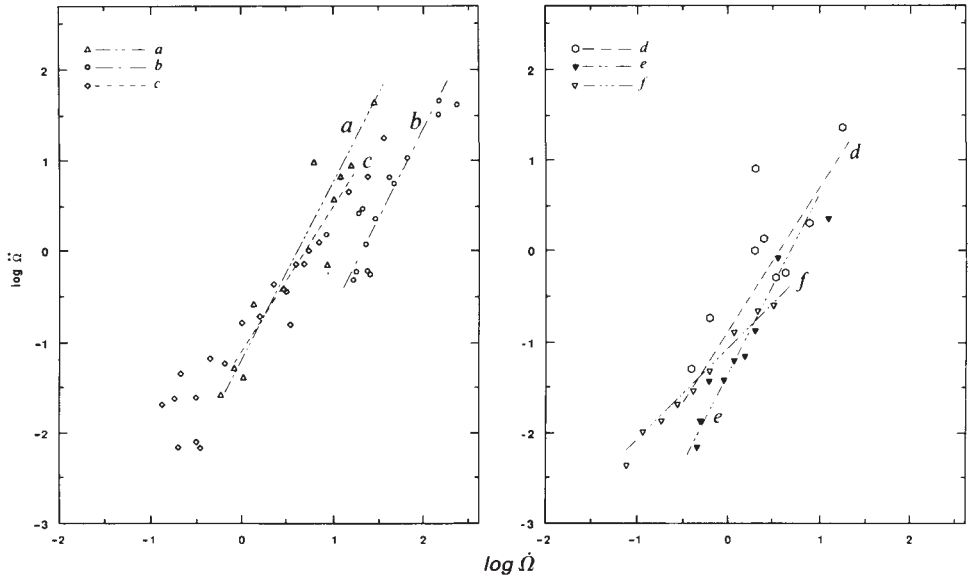

Fig. 1 Relationship between $\ddot{\Omega}$ and daily rate $\dot{\Omega}$ preceding eruption or failure, for different events and meanings of Ω. *a*, Ω = line length change (cm), Mt St Helens, 1982, $\alpha = 1.96$; *b*, Ω = tilt (μrad), Mt St Helens, 1982, $\alpha = 2$; *c*, Ω = fault movement (cm), Mt St Helens, 1981, $\alpha \simeq 1.4$; *d*, Ω = cumulative seismic strain release ($10^3 J^{1/2}$), Bezymyanny, 1960, $\alpha = 1.6$; *e*, Ω = surface movement (cm), Mt Toc, 1963, $\alpha = 1.97$; *f*, Ω = surface movement (cm), Mt Toc, 1960, $\alpha = 1$.

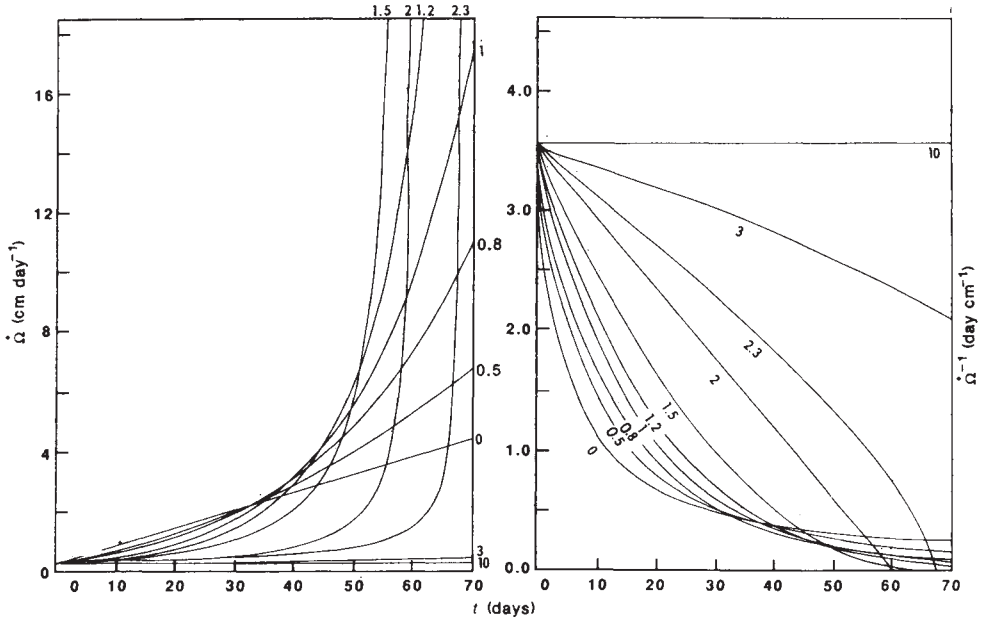

Fig. 2 Rate (left) and inverse rate (right) against time, showing curvature for different α values as indicated. Input simulates example for line length change at dome: $A = 0.059$, $\dot{\Omega}_0 = 0.28$ cm day^{-1}, $t_0 = 0$. Equation (2) for curve $\alpha = 1$; otherwise equation (3*a*). For 19 March 1982 eruption at Mt St Helens, actual $\alpha \simeq 2$.

Expressions for Ω arise from double integration of equation (1). For $\alpha = 1$,

$$\Omega - \Omega_0 = \frac{\dot{\Omega}_0}{A}(e^{A(t-t_0)} - 1) \tag{4}$$

For $\alpha = 2$, and neglecting the $\dot{\Omega}_f$ term,

$$\Omega - \Omega_0 = \frac{1}{A}[\ln(t_f - t_0) - \ln(t_f - t)] \tag{5}$$

For $\alpha > 1$, $\alpha \neq 2$,

$$\Omega - \Omega_0 = \frac{1}{A(\alpha - 2)} \times \{\dot{\Omega}_0^{2-\alpha} - [A(1-\alpha)(t - t_0) + \dot{\Omega}_0^{1-\alpha}]^{(2-\alpha)/(1-\alpha)}\} \tag{6a}$$

or

$$\Omega - \Omega_0 = \frac{1}{A(\alpha - 2)}\{[A(\alpha - 1)(t_f - t_0) + \dot{\Omega}_f^{1-\alpha}]^{(2-\alpha)/(1-\alpha)} - [A(\alpha - 1)(t_f - t) + \dot{\Omega}_f^{1-\alpha}]^{(2-\alpha)/(1-\alpha)}\} \tag{6b}$$

By manipulation of equation (3), at any arbitrary $t = t_*$, where $\dot{\Omega} = \dot{\Omega}_*$, the time to failure can be calculated:

$$t_f - t_* = \frac{\dot{\Omega}_*^{1-\alpha} - \dot{\Omega}_f^{1-\alpha}}{A(\alpha - 1)} \tag{7}$$

For $\dot{\Omega}_f$ assumed infinite

$$t_f - t_* = \frac{\dot{\Omega}_*^{1-\alpha}}{A(\alpha - 1)} \tag{8}$$

gives an upper-bound solution. Neglect of the terminal rate leads to non-conservative forecasts, but the error is often small and may not be important to decision makers.

In the analytical method using equations (7) or (8), values for A and α may be estimated from a plot such as that in Fig. 1, or from solving a set of simultaneous equations like equation (3), using rates observed up to the current time. Least-squares regression provides an estimate of error. The accuracy of the method is determined by the precision and frequency of observations and the regularity and continuity of the observed phenomena. The log rate–log time relation of Fig. 3 is useful for hindcast calculations but requires knowledge of the eruption date and cannot be used for prediction.

The time of eruption t_e is related to the time of failure t_f by $t_e = t_f + f(t)$, where $f(t)$ is an arbitrary function. This simply indicates that there can be a time delay between rupture of a conduit at depth or surficial collapse of an endogenous dome, and the venting of eruption products. Although some volcanoes may require different functions, in many cases a delay interval expressed in hours or days may be sufficient. Under other circumstances t_e may be simply equated to t_f.

The time to failure can also be ascertained graphically using the reciprocal-rate curve. Studies of the perception of curves that grow with time demonstrate that forecast accuracy is aided by inverse representation[10,11]. As large differences in such sequences occur early rather than late, trends may be recognized early. As used here, the inverse rate

$$\dot{\Omega}^{-1} = [A(1-\alpha)(t - t_0) + \dot{\Omega}_0^{1-\alpha}]^{1/(\alpha-1)} \tag{9}$$

decreases continuously with time, linearly for $\alpha = 2$, upwardly convex for $\alpha > 2$ and concave for $\alpha < 2$ (Fig. 2). Experience suggests that for volcanoes, α is frequently nearly 2. In such cases the inverse form is nearly linear[9], and graphical extrapolation is straightforward. Failure occurs when the inverse rate value $\dot{\Omega}_f^{-1}$ is obtained; for $\dot{\Omega}_f^{-1}$ neglected, failure is approximated as the point of intersection of the reciprocal rate curve with the time axis.

Both this extrapolation and equations (7) or (8) enable the prediction of specific (if often preliminary) eruption dates, rather than merely broad 'time windows' within which eruptions are considered likely. Predictions are easily updated with new data. In experienced hands, the method provides a way to improve the art of prediction at particular volcanoes, and may allow extrapolation of predictive patterns to volcanoes elsewhere.

The preceding relations apply where loading is relatively steady. For variable stress (σ), equations (2) and (3) may be expanded as follows. For $\alpha = 1$,

$$\dot{\Omega} = \dot{\Omega}_0'(\sigma/\sigma')^m e^{A(t-t_0)} \tag{10}$$

for $\alpha \neq 1$,

$$\dot{\Omega} = \{A(1-\alpha)(t - t_0) + [\dot{\Omega}'(\sigma/\sigma')^m]^{1-\alpha}\}^{1/(1-\alpha)} \tag{11a}$$

or for $\alpha > 1$,

$$\dot{\Omega} = \{A(\alpha - 1)(t_f - t) + [\dot{\Omega}_f'(\sigma/\sigma')^m]^{1-\alpha}\}^{1/(1-\alpha)} \tag{11b}$$

where $\dot{\Omega}_0'$ and $\dot{\Omega}_f'$ are initial and failure rates associated with a stress σ', and m is an empirical constant. For variable stress

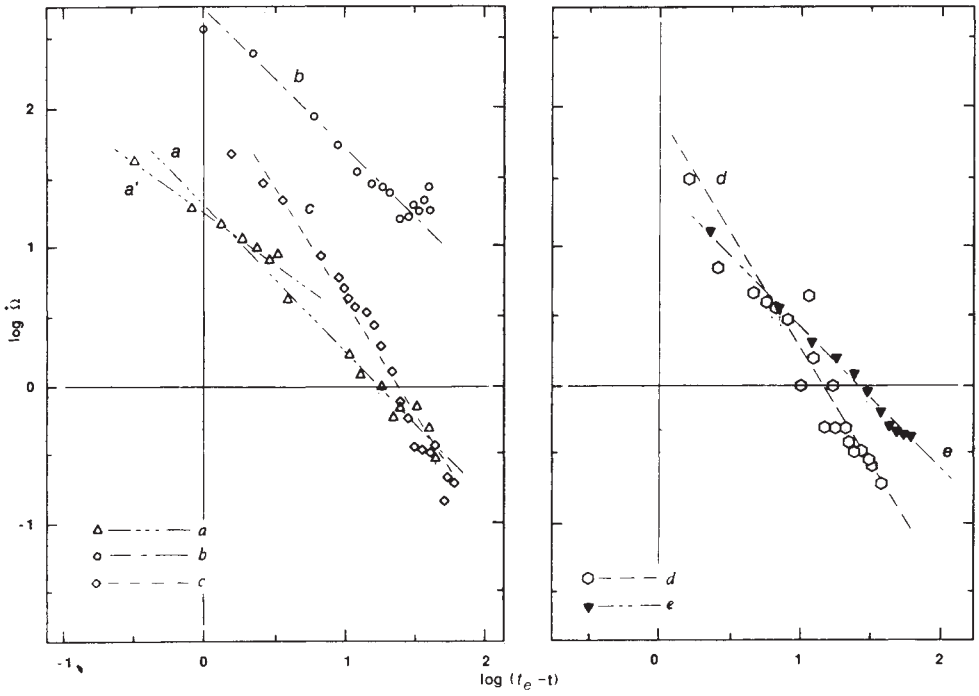

Fig. 3 Relationship between logarithm of rate and logarithm of time preceding eruption or failure. Negative slopes $n = 1/(\alpha - 1)$ for data are as follows: *a*, line length change, Mt St Helens, 1982, $n = 1.04$; *a'*, same, 3 days before eruption, $n = 0.73$; *b*, tilt, Mt St Helens, 1982, $n = 1.0$; *c*, fault, Mt St Helens, 1981, $n \simeq 1.5$; *d*, cumulative seismic strain release, Bezymyanny, $n = 1.66$; *e*, surface movement, Mt Toc, 1963, $n = 1.03$.

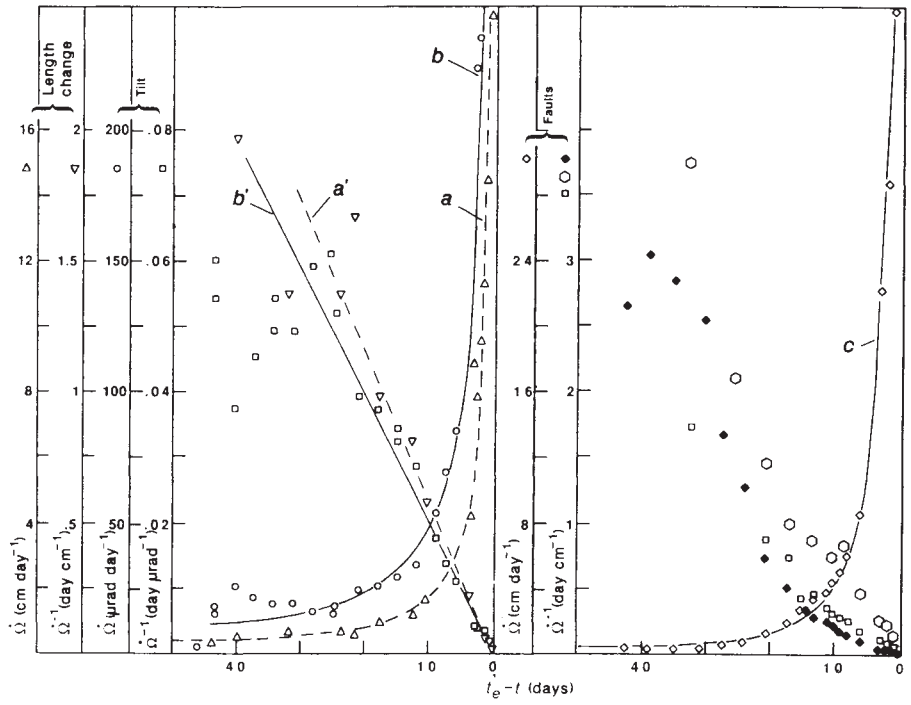

Fig. 4 Mount St Helens. Left, rates and inverse rates against time before the 19 March 1982 eruption. Ω Is line length change (curves *a*, *a'*) or tilt (*b*, *b'*), with primes indicating the inverse-rate curves. For both data sets, $\alpha = 2$. Right, Christina 2 fault movement (curve *c*, diamonds) before the September 1981 eruption, $\alpha = 1.4$. Inverse rates for two other faults indicated by squares and hexagons.

histories, failure life is governed by a life fraction rule of the type

$$\sum_{i=1}^{n} (t_i/t_f^i) = 1, \tag{12}$$

where t_i is the time over which stress σ_i is applied, and t_f^i is the rupture time corresponding to the constant stress σ_i.

Special cases encompassed by equation (1) and related expressions include many independently discovered empirical or quasi-deterministic equations that describe time-deformation relations preceding failure. Such cases, which to a certain extent provide a validation of equation (1), include the Rabotnov-Kachanov equations of materials science[12], the Monkman-Grant equation for deformation of metals and alloys[13], the general Saito expression[14-16] (developed for soils but applicable to various materials), and exponential idealizations of tertiary creep[16].

For example, the general Saito expression[15,16] for creep rate $\dot{\varepsilon}$,

$$\dot{\varepsilon} = E(t_f - t)^{-n} \tag{13}$$

is equivalent to equation (3) when $\Omega = \varepsilon$, $E = [A(\alpha - 1)]^{1/(1-\alpha)}$, $n = 1/(\alpha - 1)$, for the special case of negligible $\dot{\Omega}_f^{1-\alpha}$ and $\alpha > 1$. The expression simplifies for $\alpha = 2$ ($n = 1$). Similarly, the Monkman-Grant expression[13],

$$t_f \dot{\varepsilon}_s^q = \text{constant} \tag{14}$$

between time to fracture t_f and minimum creep rate $\dot{\varepsilon}_s$, is duplicated with equation (3) by setting $\Omega = \varepsilon$, $\dot{\varepsilon} = \dot{\varepsilon}_s$ at $t = t_0 = 0$, and neglecting $\dot{\Omega}_f^{1-\alpha}$, yielding

$$t_f \dot{\varepsilon}_s^{\alpha-1} = 1/A(\alpha - 1) \tag{15}$$

The Monkman-Grant expression is thus a special case of equation (1), for $\dot{\Omega}_f$ large and $\alpha > 1$, where $\alpha = q + 1$. Because

Monkman-Grant-type plots ordinarily employ total rupture life rather than time in tertiary creep, an adjustment in timescale may be necessary for the calculation of equivalent constants.

Applications

In the following, theory is discussed in relation to three eruptions at Mt St Helens, USA, two eruptions at Bezymyanny Volcano, USSR, and a major rockslide at Mt Toc, Italy. The examples have been chosen to illustrate the manipulation of data from diverse geodetic and seismic observations in order to provide guidance for practical applications in eruption forecasting.

Line length changes at Mount St Helens dome. On 12 March 1982 a "relatively long-term prediction" was issued for the Mount St Helens volcano, indicating that "an eruption is likely within the next three weeks"[1]. By 15 March, with greatly accelerated deformation, this prediction was updated at 19:00 PST (local time): "An eruption, most likely of the dome building type, will probably begin within 1 to 5 days." At 09:00 PST on 19 March, a "relatively short-term prediction" based on increased seismicity during the day stated that "an eruption would begin soon, probably within 24 hours". The eruption began at 19:27 PST on 19 March (see cover).

Deformation monitoring from the crater floor was critical to the "relatively long-term" predictions. Experience at Mount St Helens has shown that inflation, recognized by contraction of certain measured distances, typically begins weeks before an eruption occurs. Letting Ω = length change, data were evaluated from curve 2 of ref. 1 by graphical differentiation. Slopes were established by coordinate differences for adjacent data points and assigned to time-interval midpoints; log velocity was then plotted against $\log(t_e - t)$, where t_e is the time of eruption (Fig. 3*a*, *a'*). The surface deformation conditions here seem appropriate for the assumption $t_e = t_f$. The data are well described by equation (3) or (13), $\dot{\Omega} = 20(t_e - t)^{-1.04}$, where the rate $\dot{\Omega}$ is in cm per day, time is in days and the exponent n is equal to $1/(\alpha - 1)$. Considering Fig. 3*a* and *a'* in detail, a divergence in slope can be seen ~3 days before the eruption, with the final trend better represented by $\dot{\Omega} = 17.4(t_e - t)^{-0.73}$ (curve *a'*). Comparable information may be gained from the plot of log acceleration against log velocity (Fig. 1*a*), although the variance is larger owing to the double differentiation necessary for acceleration. The complete data set is well fit by equation (1), $\ddot{\Omega} = 0.059\dot{\Omega}^{1.96}$, an expression equivalent to $\dot{\Omega} = 20(t_e - t)^{-1.04}$.

The effect of α on rate is illustrated in Fig. 2 (left). Although for each curve an increase of rate with time seems to be relatively distinct, beyond any arbitrary point in time, it is difficult to achieve an accurate visual extrapolation of rate increase. The value $\alpha = 1.96$, however, indicates a nearly linear function of inverse rate with time (compare $\alpha = 2$ curve in Fig. 2 (right), and curve *a'* in Fig. 4). Nearly uniform decrease of the inverse rate allows graphical extrapolation of the time of eruption to be made with reasonable confidence. Alternatively, pre-eruption estimates of α and A may be used to calculate the time of eruption from equation (7) or (8).

With this method, an experienced interpreter might be able to recognize predicted eruption windows earlier than was formerly possible. Specific eruption dates could, under favourable circumstances, be targeted from the "relatively long-term" perspective—which for the 19 March example was >10 days in advance of the eruption. The method is iterative and permits sequential adjustments with new data.

Finally, accumulation of α and A values for various pre-eruptive phenomena allows experience to be quantified and perhaps applied with greater precision in future events. The efficiency of eruption prediction should be enhanced at specific volcanoes, and quantified patterns might be successfully extrapolated to volcanoes elsewhere, even if exact values are not duplicated.

Tilt measurements. Here Ω represents tilt data from Mount St Helens for the period February–March 1982, for comparison to the distance measurements for the same 19 March eruption of the previous example, and to illustrate the importance of redundancy and cross-correlation of data in eruption prediction. Both radial and tangential tilt at one station (ROA) resumed in mid-January and accelerated fairly smoothly through March[17]. A break in trend and some irregularity occurred on both curves in early to mid-February.

In curve *b* of Fig. 3, the log rate of tilt ($\dot{\Omega}$ is angular velocity, in μrad per day) is plotted against $\log(t_e - t)$. Here too the data seem to fit reasonably well the simplified form with $\alpha = 2$, less weight being accorded to the disturbed data of mid-February, corresponding to $\log(t_e - t) \simeq 1.5$. This representation gives $\dot{\Omega} = 500(t_e - t)^{-1}$, and is equivalent to $\ddot{\Omega} = 0.002\dot{\Omega}^2$, where $\ddot{\Omega}$ is angular acceleration. The latter expression is tested in Fig. 1 (curve *b*).

Actual tilt rates plotted against time in Fig. 4 (curve *b*) show a close relation to the $\alpha = 2$ approximation. In this same figure (curve *b'*), it is not surprising to see the inverse rate $\dot{\Omega}^{-1}$ descending in nearly linear fashion with time from an irregular plateau of high values. This descent seems recognizable ~18 days before the eruption. If the data had been graphically interpreted in this fashion on 12 March, when an eruption was predicted to occur "within three weeks", a narrow window of, say, 15–21 March might have been suggested. For $A \simeq 0.002(\pm 0.0005)$, application of equation (7) or (8) would have suggested initiation of eruption between 17 and 22 March.

Faults activated by a magmatic system. Several data sets can be used to produce independent α values and inverse rate against time curves. These may exhibit different negative slopes and curvatures, but ideally should converge toward a common eruption date. This concept is illustrated by 1981 data on movement of thrust faults outward from the volcanic dome at Mount St Helens[1,18]. Here Ω represents cumulative contraction of taped distances across a thrust-fault toe. As rates of observed crater-floor deformation were comparable to those preceding earlier eruptions, a "relatively long range prediction" was issued on 26 August, stating that an eruption was likely within a 2-week period starting 2 September[1]. A "relatively short-term prediction" and a revision were issued on 6 September, the day of lava extrusion. Swanson *et al.*[1] note that data were available on 3 September for an improved update of the long-term prediction.

Concave-upward curvature of the inverse rate versus time plot for the Christina 2 fault (Fig. 4 solid diamonds) indicates $\alpha < 2$. For $A \simeq 0.1$ (Fig. 1*c*), equation (8) indicates correctly the date of eruption over 10 days in advance to an accuracy of a few days. An increase of α with time is suggested by Fig. 3*c*, implying an increase in linearity of the inverse-rate curve and increasingly less ambiguous graphical extrapolation to the time of eruption.

The relationships of inverse rate to time for three independent data sets from different faults are compared in Fig. 4. Both convex and concave curvatures are displayed (implying, respectively, $\alpha > 2$ and $\alpha < 2$), but nonetheless the data points converge towards the date of actual eruption, 6 September.

Seismic energy release. Characteristics of the seismic activity of volcanoes include the energy E_s, expressed in joules, and the cumulative strain release $E_s^{1/2}$. It has been recognized that andesitic eruptions may be preceded by a systematic increase in the cumulative strain release[5,19–21]; continuous seismic monitoring may thus serve as a basis for eruption prediction. In practice, surface events may be distinguished from medium to low-frequency events, and the square root of energy release can be plotted separately for each group. Both types of event appear to increase before eruptions, but at different rates[5].

As an example[21], we consider Ω = cumulative strain release in units of $10^3\ J^{1/2}$ for the Bezymyanny, Kamchatka, eruption of 12 April 1960. The eruption date is indicated by t_e. Graphical differentiation, both from individual data and from the smoothed curve[21], yields cumulative strain rates $\dot{\Omega}$. The logarithms of these quantities are plotted against $\log(t_e - t)$ in

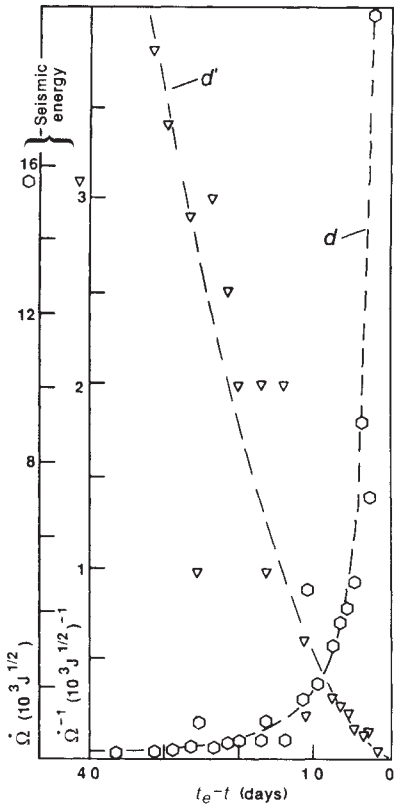

Fig. 5 Bezymyanny. Cumulative seismic strain release rate $\dot{\Omega}$ (curve d) and inverse rate $\dot{\Omega}^{-1}$ (d') against time before 12 April 1960 eruption.

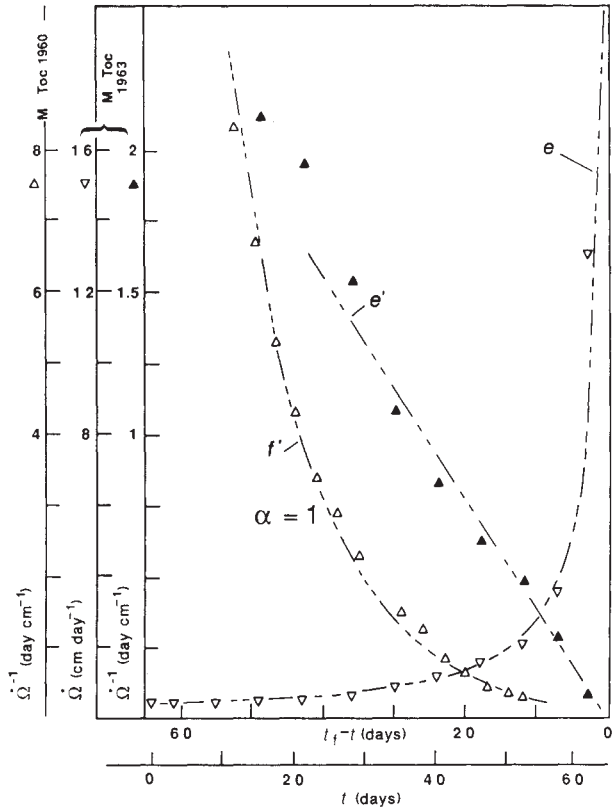

Fig. 6 Mt Toc. Displacement rate $\dot{\Omega}$ (curve e) and inverse-rate $\dot{\Omega}^{-1}$ (curve e') against time before 9 October 1963 slope failure. Exponential inverse-rate against time (curve f') for Fall 1960 movement.

Fig. 3. The distribution of data is linear and well fit by equation (3) or (13), $\dot{\Omega} = 80(t_e - t)^{-1.66}$. The equivalent expression for equation (1) is $\Omega = 0.12\dot{\Omega}^{1.6}$ (Fig. 1d).

Actual strain rates are in accord with model curves (Fig. 5), which grow rapidly as eruption impends. The inverse-rate curve is concave upwards but not emphatically so, and linear extrapolation within the 10 days preceding the eruption would have indicated the correct date of eruption to an accuracy of a few days. Thus, equation (1) shows promise of utility, in at least some circumstances, in eruption prediction with seismic quantities[22]. In some instances an appropriate delay interval of hours to days should separate the time of eruption t_e from the peak of seismic energy release denoted by t_f.

Volcanic debris avalanches and directed-blast volcanism. Anticipation of slide depth, and an estimate of the likelihood of interception of a magmatic-hydrothermal system, are essential for forecasting the possibility of blast volcanism or post-slide plinian activity associated with rockslides and avalanches from an active volcano. For such an association, the problem of predicting explosive volcanism is virtually that of predicting slide failure. This is an instance in which paroxysmal explosivity may be expected at the outbreak of an eruption. Among the most reliable and least ambiguous of observational data for prediction of the time of slope failure are displacements; instrumental extensometer and tilt measurements can provide continuous data[23]. As in 1986 at Nevado del Ruiz, Colombia, such data may make possible the forecast that slope collapse is improbable, thus reducing the concerns faced by decision makers considering evacuation and other mitigation procedures[24].

Prediction of time to slope failure may be based on velocities or on strains. In the absence of a quantitatively predicted volcanic avalanche, an example of the method is given by the 270 million cubic metre rockslide of Mt Toc, Italy—a slide volume rarely exceeded in historic times[25-28]. The 1963 slide moved a 250-m-thick rock mass 300-400 m horizontally, coming to rest after running up the opposing valley wall. Here, Ω is taken to be horizontal displacement.

A plot of log $\dot{\Omega}$ against log $(t_f - t)$ for movement data over the period 6 August to 9 October 1963 (Fig. 3e), suggest that the data are well expressed by $\dot{\Omega} = 28.8(t_f - t)^{-1.03}$, or within error limits, $\dot{\Omega} = 27(t_f - t)^{-1}$. Corresponding acceleration-velocity relationships are $\ddot{\Omega} = 0.040\dot{\Omega}^{1.97}$, or $\ddot{\Omega} = 0.037\dot{\Omega}^2$.

The velocity-time plot demonstrates the adequate fit of these expressions to the data (Fig. 6e, e'). With the inverse rate linear for $\alpha \simeq 2$, a practical prediction of the failure date could have been made in late September, more than 10 days before the actual failure on 9 October. The high velocity of the slide created a surge of water in a reservoir, overtopping a dam, killing more than 2,000 people, and causing losses totalling 200 million (1964) US dollars[25].

A special case is illustrated by an earlier movement phase, in the autumn of 1960, for which α is nearly unity (Figs 1f, 6f'). For $\alpha = 1$ the integral of equation (1) leads to a simple exponential, as confirmed by a plot of ln $\dot{\Omega}$ against time, $\dot{\Omega} = 0.042e^{0.081t}$.

On 18 May 1980, a rockslide-avalanche triggered a volcanic lateral blast at Mount St Helens, Washington[29,30]. Major lateral displacement of a sector of the cone produced extensional deformation across a kilometre of the north summit area, first observed on 27 March. This suggested that the 'toe' of a potential slide was being compressed, and the possibility of a cubic-kilometre-scale avalanche and associated catastrophic blast[31] was recognized before the start of geodetic monitoring on 23 April[32-34]. Monitoring soon indicated deformation rates of ~2 m per day on the high north flank of the cone[29,35]. A close association of earthquake foci with the bulging area led most scientists studying the volcano to conclude correctly in May that a shallow magmatic intrusion was taking place[32,33], but before 18 May

there was no scientific consensus on future expectations, and thus no "institutional judgment"[36]. Among alternative outcomes considered were the emplacement of a volcanic dome or a north-flank slide much smaller than that which occurred on 18 May[35,37].

The rate of movement was expected to increase before any actual slide detachment[35], but was never observed to occur generally except near the toe. With the available observational data, the method of inverse rate against time could not have been used to predict the occurrence of the 18 May Mount St Helens avalanche; however, a related method seems applicable.

Displacement rates were so large that, if sustained for sufficient time, slope failure was certain. This statement is equivalent to a failure criterion based on strain or total displacement, implying a relationship between rupture life and strain, such as equation (14) or (15). Based on equation (14), Saito and Uezawa[38] plotted data from compression tests on different soils, many of volcanic derivation, and reported

$$\log t_f = 2.33 - 0.916 \log \dot{\varepsilon}_s \pm 0.59 \qquad (16)$$

and a simplified form assuming an exponent of unity,

$$t_f = 214\dot{\varepsilon}_s^{-1}(\pm 0.59) \qquad (17)$$

where t_f is rupture life in minutes from the inception of loading and $\dot{\varepsilon}_s$ is minimum creep rate in units of 10^{-4} min^{-1}. Although based on laboratory experiments, equation (16) is considered applicable to full-scale slope failure[38,39]. If loading at Mount St Helens occurred at ~2 m per day over a 2 km base length; $\dot{\varepsilon}_s \simeq 0.001$ day^{-1} $\simeq 0.007 \times 10^{-4}$ min^{-1}. From equation (16), rupture is predicted within the range 4–55 days, as reckoned from very late in March[40]. The simplified form gives confidence limits of 5 to 82 days. These estimates enclose the 18 May failure of Mount St Helens, for which t_f is ~53 days.

The 30 March 1956 event at Bezymyanny, Kamchatka, provides the only other available data set for an avalanche and directed blast[41]. A 230-m horizontal displacement of the cone was detected in conjunction with dome growth, probably occurring within the period November 1955 to February 1956, suggesting an average rate of ~2.5 m per day. The minimum rate was less than this, and the base length was somewhat less than 2 km, so here too $\dot{\varepsilon}_s$ seems to be ~0.001 day^{-1}—about the same as at Mount St Helens. Predicted time to failure is thus ~5–82 days, not quite encompassing the actual time to failure at Bezymyanny of ~120 days.

As a predictor, this empirical relationship is only expected to have order-of-magnitude accuracy. Its importance is to focus attention on the inevitability of sector failure of volcanic cones within months if magmatic pressure induces sustained high rates of lateral displacement.

An improved relationship could consider such factors as scale dependency, geometry of loading, lithology, stress and movement history, equivalent viscosity of the magma, intrusion rate, and chamber or conduit geometry. The scale effect, for example, would imply that larger masses may be able to absorb larger strain before failure, consistent with the compliancy of a rock mass in comparison to compliancy of intact small specimens tested in the laboratory. Based on the two cases considered, times of failure for cone sectors of order 1 km^3 may be better approximated by $t_f = 800\dot{\varepsilon}_s^{-1}$, with an expected accuracy of perhaps 0.6 log units [that is, $\log t_f = \log(800\dot{\varepsilon}_s^{-1}) \pm 0.6$]. This relationship would predict $t_f \simeq 80$ days (range 20–320 days) for $\dot{\varepsilon}_s \simeq 0.001$ day^{-1}.

The surface motions of rock adjacent to magma could overwhelm the nearly elastic-range local motions preceding fracture growth at depth in limited parts of the system[40], and acceleration of the latter could go undetected if not specifically searched for. The possibility exists in hindsight for Mount St Helens that increased emphasis on geodetic surface monitoring in the vicinity of the toe might have revealed accelerations pertinent to evaluating stability[23]. Quasi-steady motion of rock slopes above an immobile toe should be recognized as concentrating stress near the toe; if stress concentration becomes sufficiently large, collapse of the toe could precipitate catastrophic release of the entire slope and trigger off a directed blast.

This work has benefited from my experience with the US Geological Survey, particularly at Cascades Volcano Observatory, from US A.I.D.-supported tasks concerning volcano hazard mitigation in Colombia and the Philippines, and from invited travel to National Research Centers for Disaster Prevention in Japan. I thank R. Janda, R. Decker, C. Newhall, D. Swanson, T. Nakamura, S. Okuda, S. Oyagi, M. Calvache, N. Banks, S. Malone, D. Dzurisin, T. Casadevall, A. Swan, R. Dionne, J. Dutton and P. Luckie, among others, for stimulation of thought, hospitality or assistance; J. Ewart for checking the mathematics; and R. L. Christiansen for a constructive review.

Received 20 July 1987; accepted 18 January 1988.

1. Swanson, D. A. *et al. Science* **221**, 1369–1376 (1983).
2. Voight, B. *Eos* **68**, 1551 (1987).
3. Voight, B. *Eos* **68**, 1286 (1987).
4. Weaver, C. S. *et al. Science* **221**, 1391–1394 (1983).
5. Malone, S. *et al. Science* **221**, 1376–1378 (1983).
6. Tazieff, H. in *Forecasting Volcanic Events* (eds Tazieff, H. & Sabroux, J.-C.) Ch. 21 (Elsevier, Amsterdam, 1983).
7. Casadevall, T. *et al. Science* **221**, 1383–1385 (1983).
8. Fukuzono, T. & Terashima, H. *Rep. natn. Res. Center Disaster Prev.* **29**, 103–122 (1982).
9. Fukuzono, T. in *Proc. 4th Natl. Conf. Field Workshop on Landslides* 145–150 (Disaster Research Institute, Kyoto, 1985).
10. Timmers, H. & Wagenaar, W. A. *Percept. Psychophys.* **21**, 558–562 (1977).
11. Wagenaar, W. A. in *Environmental Assessment of Socioeconomic Systems* (eds Burkhardt, D. F. & Ittelson, W. H.) (Plenum, New York, 1978).
12. Leckie, F. A. in *Mechanics of Engineering Materials* (eds Desai, C. S. & Gallagher, R. H.) Ch. 21 (Wiley, New York, 1984).
13. Monkman, F. C. & Grant, N. J. *Proc. Am. Soc. Test. Mater.* **56**, 593–605 (1956).
14. Saito, M. *Proc. 7th int. Conf. Soil Mech. Found Engng* **2**, 677–683 (1969).
15. Yamaguchi, S. *Rep. Sogu Doboku Lab.* No. 14 (Tokyo, 1978).
16. Varnes, D. J. *Proc. 7th Southeast Asian geotech. Conf.* **2**, 107–130 (1983).
17. Dzurisin, D. *Science* **221**, 1381–1383 (1983).
18. Chadwick, W. W. Jr *et al. Science* **221**, 1378–1380 (1983).
19. Tokarev, P. I. *Eruptions and Seismic Regime of Klyuchevskaya Group Volcanoes*, (Nauka, Moscow, 1966) (in Russian).
20. Tokarev, P. I. *Dokl. Akad. Nauk SSSR* **199**, 422–425 (1971).
21. Tokarev, P. I. in *Forecasting Volcanic Events* (eds Tazieff, H. & Sabroux, J.-C.) Ch. 19 (Elsevier, Amsterdam, 1983).
22. Wu, F. T. & Thomson, L. *Int. J. Rock Mech. Min. Sci. Geomech. Abstr.* **12**, 167–173 (1975).
23. Voight, B. *Eos* **68**, 456 (1987).
24. Voight, B. *et al.* in *Proc. 6th Congr. int. Soc. Rock Mechanics* (eds Horget, G. & Vongpaisal, S.) pp. 275–279 (A. A. Balkema, Rotterdam, 1987).
25. Muller, L. *Rock Mech. engng Geol.* **2**, 148–212 (1964).
26. Selli, R. & Trevisan, L. *Annali del Museo Geologico di Bologna* **32**, 8–104 (1964).
27. Hendron, A. J. Jr & Patton, F. D. *Geotechnical Laboratory tech. Rep.* No. GL-85-5 (U.S. Army Engineer exp. Sta., Vicksburg, 1985).
28. Voight, B. & Faust, C. *Géotechnique* **32**, 43–54 (1982).
29. Voight, B. *et al. Géotechnique* **33**, 243–273 (1983).
30. Voight, B. *et al. Prof. Pap. U.S. geol. Surv.* **1250**, 347–377 (1981).
31. Voight, B. Slope stability hazards, Mt St Helens Volcano, Washington. *Tech. Rep. U.S. geol. Surv.* File report, Cascades Volcano Observatory, Washington (1980).
32. Decker, R. W. *Prof. Pap. U.S. geol. Surv.* **1250**, 815–820 (1981).
33. Decker, R. W. *A. Rev. Earth planet. Sci.* **14**, 267–291 (1986).
34. West, S. *Science News* **118**, 399 (1980).
35. Lipman, P. W. *et al. Prof. Pap. U.S. geol. Surv.* **1250**, 143–156 (1981).
36. Wesson, R. L. *Yb. U.S. geol. Surv.*, FY 1980 (1982).
37. Miller, D. *et al. Prof. Pap. U.S. geol. Surv.* **1250**, 789–802 (1981).
38. Saito, M. & Uezawa, H. *Proc. 5th int. Conf. Soil Mech.* **1**, 315–318 (1961).
39. Saito, M. *Proc. 6th int. Conf. Soil Mech. Found. Engng* **2**, 537–541 (1965).
40. Voight, B. in *Proc. int. Conf. Landslides.* State-of-art (oral) report, Toronto (1984).
41. Gorshkov, G. S. *Bull. volcan.* **20**, 77–109 (1959).